

Jamming Resilient Indoor Factory Deployments: Design and Performance Evaluation

Leonardo Chiarello^{*§}, Paolo Baracca[§], Karthik Upadhy[†],
Saeed R. Khosravirad[‡], Silvio Mandelli[§], and Thorsten Wild[§]
^{*}Department of Information Engineering, University of Padova, Italy
[§]Nokia Bell Labs, Stuttgart, Germany
[†]Nokia Bell Labs, Espoo, Finland
[‡]Nokia Bell Labs, Murray Hill, USA

Abstract—In the framework of 5G-and-beyond Industry 4.0, jamming attacks for denial of service are a rising threat which can severely compromise the system performance. Therefore, in this paper we deal with the problem of jamming detection and mitigation in indoor factory deployments. We design two jamming detectors based on pseudo-random blanking of subcarriers with orthogonal frequency division multiplexing and consider jamming mitigation with frequency hopping and random scheduling of the user equipments. We then evaluate the performance of the system in terms of achievable block error rate (BLER) with ultra-reliable low-latency communications traffic and jamming missed detection probability. Simulations are performed considering a 3rd Generation Partnership Project spatial channel model for the factory floor with a jammer stationed outside the plant trying to disrupt the communication inside the factory. Numerical results show that jamming resiliency increases when using a distributed access point deployment and exploiting channel correlation among antennas for jamming detection, while frequency hopping is helpful in jamming mitigation only for strict BLER requirements.

Index Terms—5G, 6G, URLLC, jamming detection, physical layer security, Industry 4.0

I. INTRODUCTION

Security has been one of the main drivers in the design of the fifth generation (5G) of mobile communication systems by the 3rd Generation Partnership Project (3GPP). In fact, 5G provides several security measures at higher layers to guarantee authentication, privacy and data integrity [1]. Moreover, radio jamming by a malicious device has also been recognized as an important type of security attack that can threaten the performance of a 5G deployment, in particular in Industry 4.0 scenarios. Despite the very affordable cost with a starting price of a few hundred dollars [2], some of these devices can be quite advanced and smart, e.g., the so-called reactive jammers [3], as capable to sense the channel and remain quiet until an ongoing legitimate transmission is detected. In fact, ultra-reliable low-latency communications (URLLC) are inherently more susceptible to the interference impact of such a denial of service attack due to their stringent quality of service requirements. For instance, a jammer stationed outside a factory that disrupts the communication among the devices inside the plant can cause large economic losses to the factory owner if production needs to be stopped. Furthermore,

handling jamming attacks has already been recognized as a very relevant theme also for sixth generation (6G) technologies [4], with physical layer security expected to play an important role in future mobile networks [5].

A jamming resilient communication system must provide both a) detection, to discriminate between the presence of a jammer and legitimate interference, and b) mitigation capabilities, to limit the caused damage by applying ad-hoc techniques. Non-reactive jammers can be detected by monitoring basic statistics like the received signal strength or the carrier sensing time, whereas the detection of smart jammers require advanced techniques combining several statistics [6]. In [7] authors propose a detection technique based on pseudo-random hopping of the scheduled user equipments (UEs) among the pilot sequences and the application of a jamming-resilient combiner exploiting massive multiple-input multiple-output (MIMO) base stations. In our previous work [8], we proposed a novel method to detect smart jamming attacks based on pseudo-random blanking of subcarriers with orthogonal frequency division multiplexing (OFDM). Regarding the mitigation problem, several schemes have already been studied, for instance applying beamforming, direct sequence spread spectrum, and power control [9]. In fact, once a jammer is detected and characterized, an off-the-shelf interference management scheme can be applied tailoring it to the specific scenario, e.g., with beamforming creating nulls toward a jammer whose channel can be estimated in the detection phase.

In this paper we extend the jamming detection proposal in [8] by providing realistic performance evaluations that consider indoor factory deployments with 3GPP spatial channel model. Moreover, we propose a new detector that exploits antenna correlation at the receiver. Finally, we consider jamming mitigation techniques with frequency hopping and random scheduling of the UEs. The benefits of the proposed schemes are evaluated in terms of jamming detection probability and block error rate (BLER) performance with URLLC.

Notation. We use $(\cdot)^H$ to denote conjugate transpose. $\|\mathbf{x}\|$ indicates the norm of vector \mathbf{x} . $|\cdot|$ denotes the absolute value. $[\mathbf{x}]_n$ is the n -th entry of vector \mathbf{x} . $F_X^{-1}(x)$ denotes the inverse of the cumulative distribution function (CDF) of the random variable (r.v.) X evaluated at x .

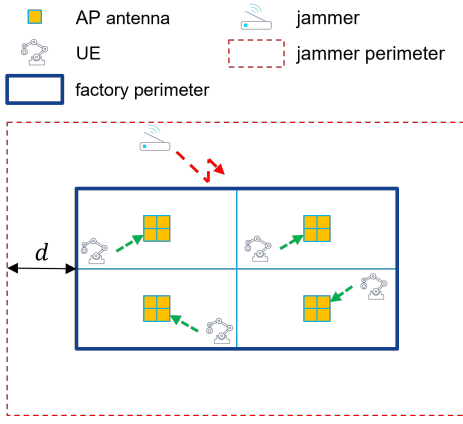


Fig. 1. Representation of the considered uplink scenario for the partially distributed deployment ($N_{\text{AP}} = 4$) and a total of $N_{\text{ant}} = 16$ antennas.

II. SYSTEM MODEL

We consider an industrial scenario as in Fig. 1 with a factory hall of dimensions $100 \times 50 \times 6$ m, and with N_{AP} access points (APs) mounted on the factory ceiling. For a fair comparison among different deployments, we consider in the whole factory a total of N_{ant} omni-directional antennas so that each AP is equipped with a square antenna array with $N_{\text{ant}}^{(\text{AP})} = N_{\text{ant}}/N_{\text{AP}}$ antennas. The following AP deployments are compared [10]:

- *Centralized deployment*: $N_{\text{AP}} = 1$ AP placed at the center of the factory hall;
- *Partially distributed deployment*: $N_{\text{AP}} = 4$ APs located such that the inter-AP distance (IAD) along the longest side is 50 m and the IAD along the shortest side is 25 m. An example of this deployment is reported in Fig. 1.
- *Fully distributed deployment*: $N_{\text{AP}} = 16$ APs located such that the IAD along the longest side is 25 m and the IAD along the shortest side is 12.5 m.

We have N_{UE} UEs active and each UE is randomly dropped within the factory at an height of 1.5 m, is equipped with a single omni-directional antenna, and transmits with power $P_{\text{UE}} = 10$ dBm.

We assume a system operating at a central carrier frequency of $f_c = 3.75$ GHz. Regarding the channel model, we consider the proposal in [11], where the 3GPP indoor office (InO) model is used as starting point and path-loss, shadowing, and line of sight (LOS) probability values are chosen on the basis of extensive measurements done in two different operational factories. This novel indoor industrial (InI) model encompasses different scenarios and here we consider the dense factory clutter model with clutter-embedded APs (more details in [11, Tab. 3]).

A. Numerology and resource allocation

We adopt an OFDM modulation compliant to the 5G numerology with 60 kHz subcarrier spacing. The subcarriers are grouped into physical resource blocks (PRBs), each consisting of $N_{\text{sc}} = 12$ consecutive subcarriers over a transmission interval of $N_{\text{symb}} = 14$ OFDM symbols [1]. Therefore, each

PRB consists of $N_{\text{RE}}^{(\text{PRB})} = N_{\text{sc}} \cdot N_{\text{symb}} = 168$ resource elements (REs) and has a bandwidth of $B_{\text{PRB}} = 720$ kHz. We consider two scenarios for our system: a total bandwidth of $B = 20$ MHz (with a total number of PRBs $N_{\text{PRB}} = 25$) with $N_{\text{UE}} = 4$ UEs, and a total bandwidth of $B = 100$ MHz ($N_{\text{PRB}} = 125$) with $N_{\text{UE}} = 20$ UEs: in both cases we set the guard band to be 10% of B . We assume URLLC traffic, such that each UE transmits a small packet of size $C = 20$ bytes in each slot, with no retransmission opportunities because of the tight latency constraint. We consider a resource allocation where interference among the active UEs is managed by allocating different UEs on different PRBs, i.e., the only interference source in the system is the jammer. The PRBs available for data transmissions are then evenly shared among the UEs, that apply equal power allocation on them. More details about the allocation of UEs to PRBs is part of the jamming mitigation strategy and will be described in Section III.

B. Jammer model

We consider an attacker stationed outside the factory at height of 1.5 m and dropped randomly within a rectangular perimeter with sides $d = 10$ m far from the factory walls (see Fig. 1). The jammer is equipped with a single omni-directional antenna element that transmits with power P_j , ranging from 20 dBm to 60 dBm [2]. Moreover, we assume the jammer to allocate equal power on the attacked PRBs and consider both a) a wide-band jammer that attacks the whole bandwidth and b) a narrow-band jammer attacking a few PRBs but with stronger power spectral density. Finally, we assume for the jammer the same InI channel model as for the UEs inside the factory, but adding a factory wall penetration loss modelled as a Gaussian r.v. $\text{PL}_{\text{wall}} \sim \mathcal{N}(\mu_P, \sigma_P^2)$, with mean $\mu_P = 27.5$ dB and standard deviation $\sigma_P = 6.5$ dB [12, Tab. 7.4.3-2].

C. Imperfect channel state information (CSI)

We assume a time division duplex (TDD) setup with pilot sequence length $T = 16$ [10]. Note that here we have no pilot contamination as different UEs are scheduled on different PRBs, but jamming affects channel estimation. Let $\mathbf{h}_{i,j}$ be the $(1 \times N_{\text{ant}}^{(\text{AP})})$ -dimensional channel vector from the i -th UE to the j -th AP on a certain PRB, with $i = 1, \dots, N_{\text{UE}}$, and $j = 1, \dots, N_{\text{AP}}$. The minimum mean squared error (MMSE) estimate $[\hat{\mathbf{h}}_{i,j}]_n$ of $[\mathbf{h}_{i,j}]_n$ can be defined as [10, Eq. (6)]:

$$[\hat{\mathbf{h}}_{i,j}]_n = \frac{\gamma_{i,j} T}{1 + \gamma_{i,j} T} ([\mathbf{h}_{i,j}]_n + z_i), \quad (1)$$

where $\gamma_{i,j} = \frac{P_{\text{UE},i}^{(\text{PRB})} \sigma_{h_{i,j}}^2}{\sigma_w^2}$ is the signal to noise ratio (SNR) of UE i at AP j and $z_i \sim \mathcal{CN}(0, (\sigma_w^2 + P_j^{(\text{PRB})} \sigma_{h_{i,j}}^2) / (P_{\text{UE},i}^{(\text{PRB})} T))$ is a complex Gaussian r.v. representing noise and interference on channel estimation. In particular, $P_{\text{UE},i}^{(\text{PRB})}$ is the power of UE i allocated to a single PRB, $\sigma_{h_{i,j}}^2$ denotes the large-scale fading attenuation between UE i and AP j , and σ_w^2 is the noise statistical power on a single PRB, computed considering a noise figure of 7 dB at the receiver. Moreover, $P_j^{(\text{PRB})}$ is the

jammer power allocated to a single PRB and $\sigma_{h_{j,j}}^2$ is the large-scale fading attenuation between the jammer and AP j .

D. Beamforming at the receiver

At the receiver, we assume joint reception (JR), such that the signals received by the APs are combined in a central unit. Since there is no interference among the active UEs in our framework, because they are scheduled on different subbands, we adopt maximum ratio combining (MRC), that maximizes the UE SNR and is easy to implement in a distributed MIMO setup. We denote with $\hat{\mathbf{h}}_i = [\hat{\mathbf{h}}_{i,1}, \hat{\mathbf{h}}_{i,2}, \dots, \hat{\mathbf{h}}_{i,N_{\text{AP}}}]$ the $(1 \times N_{\text{ant}})$ -dimensional vector collecting the estimated channels between the i -th UE and all the APs. The MRC beamforming is then defined as:

$$\mathbf{g}_i = \hat{\mathbf{h}}_i^H / \|\hat{\mathbf{h}}_i\|. \quad (2)$$

E. System key performance indicators (KPIs)

In order to quantify the impact of the jammer to the system, we introduce two KPIs: signal to interference plus noise ratio (SINR) on data transmission and BLER. We define the SINR of UE i on a certain PRB, whose index is skipped for the sake of clarity, as

$$\text{SINR}_i = \frac{|\mathbf{h}_i \mathbf{g}_i|^2 P_{\text{UE},i}^{(\text{PRB})}}{\sigma_w^2 + |\mathbf{h}_j \mathbf{g}_i|^2 P_j^{(\text{PRB})}}, \quad (3)$$

where at the denominator we have the malicious interference from the jammer, with \mathbf{h}_j the $(1 \times N_{\text{ant}})$ -dimensional channel vector collecting the channels between the jammer and all the AP antennas.

We assume that UE i sends its packet over F_i PRBs and define $C_{\text{cod},i} = F_i \cdot N_{\text{RE}}^{(\text{PRB})}$ as the number of REs allocated to that packet. Then, for our analysis, we use the exponential effective SINR metric (EESM) as link-to-system mapping criterion [13, Eq. (3)] to compute, as a function of the different SINRs (3) experienced by a certain UE on different PRBs, a single $\text{SINR}_{\text{pkt},i}$, that represents the equivalent SINR for the packet. We then use this $\text{SINR}_{\text{pkt},i}$ to compute the BLER of UE i from the normal approximation of the finite blocklength capacity [14, Eq. (5)]:

$$\text{BLER}_{\text{pkt},i} = Q\left(\left[\log_2\left(1 + \text{SINR}_{\text{pkt},i}\right) - \rho_i + \frac{\log_2 \tilde{C}_{\text{cod},i}}{2\tilde{C}_{\text{cod},i}}\right] \sqrt{\frac{\tilde{C}_{\text{cod},i}}{V}}\right), \quad (4)$$

where V is the channel dispersion [14, Eq. (8)], $\rho_i = C/\tilde{C}_{\text{cod},i}$ is the spectral efficiency for the UE i packet, and $\tilde{C}_{\text{cod},i} = C_{\text{cod},i}(1 - O)$ is the coded packet size in REs taking into account the system overhead $O = 0.25$ for control and pilots.

III. DEFENSE STRATEGY

In this work we consider the defense strategy framework for performing jamming detection that we initially proposed in [8], where some PRBs in each slot are blanked in a pseudo-random manner, such that the attacker cannot predict in advance which resources will be used for transmission and which will be blanked. In detail, in each slot all the UEs blank a set $\mathcal{M}_P \subset \{1, \dots, N_{\text{PRB}}\}$ (with cardinality $M_P = |\mathcal{M}_P|$) of PRBs, where the set elements are chosen in a pseudo-random manner; the remaining PRBs are used for data transmission. At the same time, the attacker transmits on a set $\mathcal{L}_P \subseteq \{1, \dots, N_{\text{PRB}}\}$ (with cardinality $L_P = |\mathcal{L}_P|$) of PRBs, where the set elements are chosen according to the jammer strategy. In this work we assume that the jammer chooses the attacked PRBs pseudo-randomly and it evenly splits its power among them. Moreover, for the sake of notation, when $L_P = N_{\text{PRB}}$ we refer to the attacker as a wide-band jammer, otherwise we call it narrow-band jammer.

A. Jamming detection strategies

The detection strategy takes advantage of the blanked PRBs to detect the presence of jamming by means of statistical hypothesis testing [15]. Moreover, we assume that jamming detection is performed by a central unit collecting the signals received from all the APs distributed in the factory hall. The two hypotheses for the sequence of blanked PRBs are as follows:

- There is no jamming and we have just thermal noise (null hypothesis \mathcal{H}_0);
- There is jamming (alternative hypothesis \mathcal{H}_1).

The above hypotheses translate to the following hypothesis test:

$$\begin{cases} \mathcal{H}_0 : \mathbf{r} = \mathbf{w} \\ \mathcal{H}_1 : \mathbf{r} = \mathbf{w} + \mathbf{j} \end{cases}, \quad (5)$$

where \mathbf{r} , \mathbf{w} , and \mathbf{j} are $((N_{\text{RE}} \cdot N_{\text{ant}}) \times 1)$ -dimensional vectors, with $N_{\text{RE}} = M_P \cdot N_{\text{RE}}^{(\text{PRB})}$, containing the samples of the blanked REs of all the antennas. In particular, \mathbf{r} is the total received signal by the APs, \mathbf{w} is the noise vector with elements $[\mathbf{w}]_n \sim \mathcal{CN}(0, \sigma_w^2/N_{\text{RE}}^{(\text{PRB})})$, and \mathbf{j} is the jamming signal with unknown distribution. Then, the test decides for \mathcal{H}_1 if

$$T(\mathbf{r}) > \delta, \quad (6)$$

where $T(\mathbf{r})$ is the test statistic and δ is the threshold, which depends on the test statistic and is function of a target false alarm (FA) probability P_{FA} , i.e., the probability of declaring jamming even if it is not present. Then, in Section IV we will evaluate the effectiveness of the proposed detection technique against a Gaussian jammer in terms of missed detection (MD) probability P_{MD} , i.e., the probability of declaring no-jamming even if it is present. Note that with (5) we perform jamming detection in each slot: however, the proposed scheme can be applied, depending on the use case, also to multiple slots for improved performance. Regarding the test statistic, we now propose two options.

1) *Generalized likelihood ratio test (GLRT)*: This test defines the test statistic simply as [8]

$$T_{\text{GLRT}} = \frac{\|\mathbf{r}\|^2}{N_{\text{RE}} \cdot N_{\text{ant}}}, \quad (7)$$

which is an energy detector. The threshold for this detector is derived as

$$\delta_{\text{GLRT}} = F_{T_{\text{GLRT}}(\mathbf{r}; \mathcal{H}_0)}^{-1}(1 - P_{\text{FA}}), \quad (8)$$

where $T_{\text{GLRT}}(\mathbf{r}; \mathcal{H}_0) \sim \text{Gamma}\left(N_{\text{RE}} \cdot N_{\text{ant}}, \frac{\sigma_w^2/N_{\text{RE}}^{(\text{PRB})}}{N_{\text{RE}} \cdot N_{\text{ant}}}\right)$ is the test statistic distribution under \mathcal{H}_0 , with $\text{Gamma}(k, \theta)$ being the gamma distribution with shape parameter k and scale parameter θ . The main advantage of this detector is the very low computational complexity, as just the received power on the blanked PRBs needs to be computed.

2) *Roy's largest root test (RLRT)*: Differently from the GLRT, this test exploits the channel correlations among the AP antennas. For deriving the test statistic, we follow the following procedure:

- 1) We denote with \mathbf{r}_m , $m = 1, 2, \dots, N_{\text{RE}}$ the column vector collecting the entries of \mathbf{r} received by all antennas on RE m .
- 2) We define $\mathbf{R} = [\mathbf{r}_1, \dots, \mathbf{r}_{N_{\text{RE}}}]$, which is a $(N_{\text{ant}} \times N_{\text{RE}})$ -dimensional matrix.
- 3) We compute the sample covariance matrix as $\mathbf{C} = \frac{1}{N_{\text{RE}}} \mathbf{R} \mathbf{R}^H$.
- 4) We define the test statistic as [16]

$$T_{\text{RLRT}} = \frac{\lambda}{\sigma_w^2}, \quad (9)$$

where λ is the largest eigenvalue of \mathbf{C} .

The threshold for this detector is derived as

$$\delta_{\text{RLRT}} \approx \mu + \xi \cdot F_{\text{TW2}}^{-1}(1 - P_{\text{FA}}), \quad (10)$$

where TW2 is the Tracy-Widom distribution of 2nd order, while μ and ξ depend on N_{ant} and N_{RE} . In particular, authors in [16] show that the approximation holds for $N_{\text{ant}}, N_{\text{RE}} \rightarrow \infty$.

When compared to the GLRT, with this detector we exploit the spatial correlation among antennas. The computational complexity increases, but is still very low as we just need to compute an eigenvalue. A second potential disadvantage is that the approximation in (10) creates a mismatch between empirical and target FA probabilities. Therefore, in order to evaluate the impact of this mismatch, in Fig. 2 we show the empirical FA probability derived in an authentic scenario, i.e., a scenario without jamming, versus the target FA probability, for a factory with $N_{\text{ant}} = 16$ antennas. Three different curves are displayed: a theoretical one, for which the two probabilities coincide, and two empirical curves corresponding to $N_{\text{RE}} = 168, 840$ (i.e., $M_P = 1, 5$). As we can see, both the empirical curves are close to the theoretical one, meaning that the approximation (10) holds very well even with realistic low values of N_{ant} and N_{RE} .

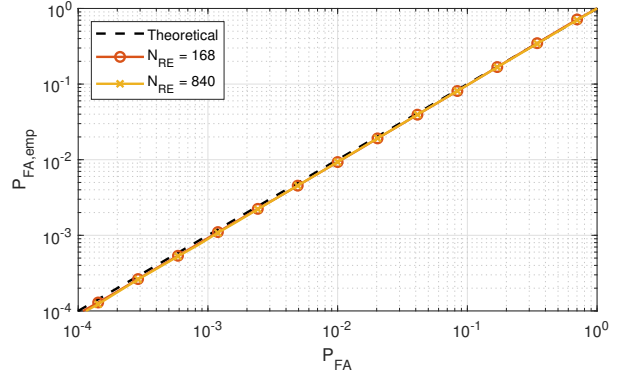


Fig. 2. Empirical FA probability versus target FA probability for $N_{\text{ant}} = 16$.

B. Jamming mitigation strategies

Alongside the above detection strategy, we consider two jamming mitigation schemes designed for narrow-band attacks: one based on user scheduling and the other one exploiting the pseudo-random blanking concept.

In Section IV we will assume *sequential scheduling* as baseline, such that adjacent PRBs are allocated to each active UE. As a first mitigation strategy, we consider *random scheduling*, where PRBs are allocated to each UE in a pseudo-random way, with the constraint that still, as introduced in Section II-A, a PRB is allocated to just one active UE, to guarantee orthogonality among UEs. The purpose of this approach is to counteract smart jammers that can learn allocation and, for instance, focus their attack on a specific subband that is used by just one or few UEs. With this method then the jammer cannot know in advance which UE will be scheduled on each PRB.

As a second mitigation strategy, we consider *frequency hopping*, where in each slot just a small number of PRBs is used for transmission, and that is implemented in our framework by greatly increasing the number of blanked PRBs M_P . The main objective is to lower the probability of intersection between jammed and data PRBs, so advantages of frequency hopping are expected with narrow- rather than wide-band jammers. When using a large number of blanked PRBs, the same packet needs to be transmitted on a lower number of data PRBs but with higher power per PRB, i.e., a higher packet spectral efficiency is needed in (4), but higher SINR is also experienced on those data PRBs: that, in fact, can be beneficial in certain interference conditions. Moreover, a large number of blanked PRBs has the benefit of performing jamming detection on more resources, thus decreasing the MD probability.

IV. NUMERICAL RESULTS

In this section we show the numerical results obtained by performing Monte Carlo simulations of the above described system. In particular, we focus on the system KPIs degradation caused by the jammer and on the MD probability of the attacker. If not otherwise specified, the following parameters are used for the simulations: $N_{\text{ant}} = 64$ antennas, high power

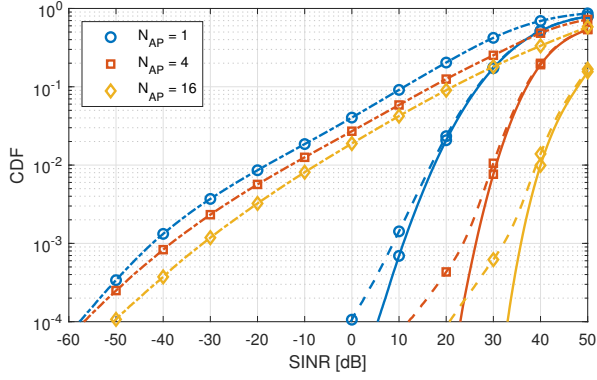


Fig. 3. CDF of SINR for $B = 20$ MHz and $L_P = 25$. Continuous lines are without jamming, dashed lines for $P_J = 20$ dBm, and dash-dotted lines for $P_J = 60$ dBm.

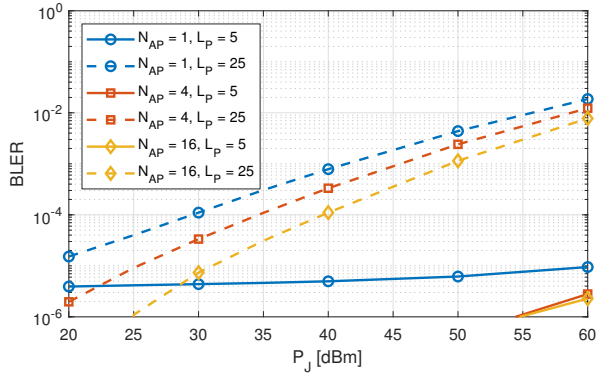


Fig. 4. BLER versus P_J for $B = 20$ MHz.

jammer with $P_J = 60$ dBm, $M_P = 5$ blanked PRBs, and random scheduling of UEs.

Fig. 3 shows the CDF of the SINR for $N_{AP} = 1, 4, 16$, $B = 20$ MHz, $P_J = 20, 60$ dBm (low- and high-power jammer), and $L_P = 25$ (wide-band jammer). Moreover, the SNR curves are also shown, representing a jamming free scenario. First, we notice as expected that the SINR is higher in the distributed deployments, i.e., with higher N_{AP} , because some of the AP antennas are closer to the UEs. On the other hand, with jamming the SINR gap among the deployments is reduced when compared to the jamming free scenario: that happens because some of the AP antennas are, with the distributed approaches, also closer to the jammer stationed outside the factory. Finally, we observe that, while on the median the SINR is still quite high even with a high-power jammer, on lower quantiles the SINR is strongly affected, for instance with about 50 dB loss at the 1st percentile, i.e., considering a CDF value of 0.01, with $N_{AP} = 16$.

To evaluate the performance degradation with URLLC type of traffic, Fig. 4 shows the BLER (4) as a function of P_J for $N_{AP} = 1, 4, 16$, $B = 20$ MHz, and $L_P = 5, 25$ (narrow- and wide-band jammer). Better BLER is achieved by the distributed deployments. Moreover, we observe that the wide-

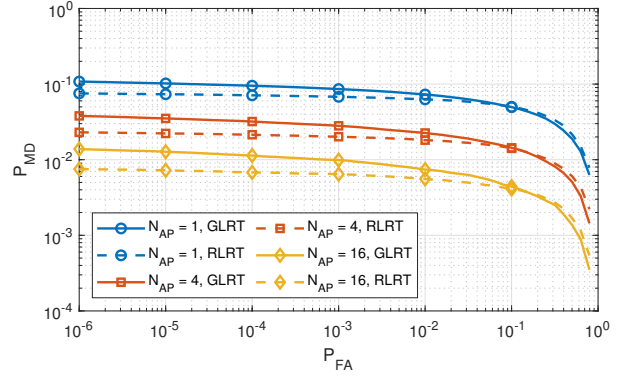


Fig. 5. P_{MD} versus P_{FA} for $B = 20$ MHz and $L_P = 25$.

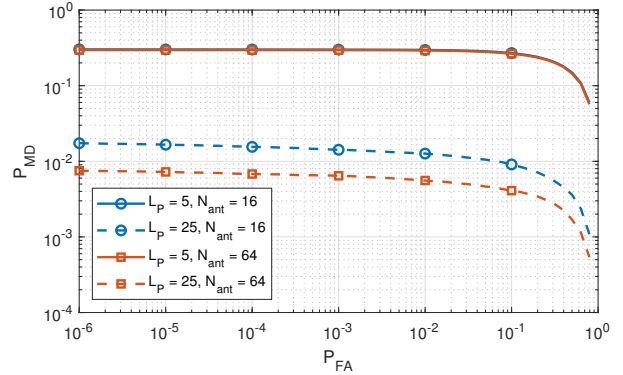


Fig. 6. P_{MD} versus P_{FA} for $N_{AP} = 16$, $B = 20$ MHz, and RLRT detector.

band attack is much more harmful than the narrow-band attack, and a huge BLER degradation is observed with a wide-band jammer: for instance, BLER increases with $N_{AP} = 4$ from about 10^{-6} to 10^{-2} when we increase the jamming power from 20 dBm to 60 dBm.

Regarding the performance evaluation of the defense strategy, Fig. 5 shows the MD probability as a function of the FA probability, a.k.a. receiver operating characteristic (ROC) curve, for $B = 20$ MHz, $L_P = 25$, and comparing GLRT against RLRT detectors. The first thing to notice is that the MD probability is lower, i.e., better, in the distributed approaches because AP antennas are closer to the jammer. Then, MD probability is slightly lower with the RLRT detector for relevant values of FA probability, confirming that exploiting spatial correlation among antennas brings benefit to the detection.

In Fig. 6 we show the ROC curve for $N_{AP} = 16$, $B = 20$ MHz, $N_{ant} = 16, 64$, $L_P = 5, 25$, and RLRT detector. Lower MD probability is achieved with more AP antennas. On the other hand, in the narrow-band case MD probability is high and similar for different number of antennas, because limited by the probability of intersection between blanked and jammed PRBs.

As last result regarding the detection performance, in Fig. 7 we report the ROC curve for $N_{AP} = 16$, $B = 100$ MHz, $M_P = 5, 85$, $L_P = 5, 25, 125$ (very narrow-band, narrow-

V. CONCLUSIONS

In this paper we considered the problem of jamming attacks in 5G-and-beyond indoor factory deployments. We a) provided extensive simulations in a realistic scenario of a factory hall with 3GPP spatial channel model and a jammer stationed outside the plant, b) proposed and compared two detectors based on pseudo random blanking of subcarriers, and c) evaluated random scheduling and frequency hopping as jamming mitigation strategies. Numerical results show that a high-power jammer can strongly degrade BLER with URLLC. As promising countermeasures, a distributed deployment is more jamming resilient than a centralized one, and the RLRT detector is capable to provide good jamming detection performance by exploiting channel correlations among the deployed antennas. Finally, frequency hopping is beneficial in mitigating jamming attacks only with narrow-band jammers and with more strict reliability requirements. Future works will include more advanced mitigation schemes exploiting MIMO and multi-connectivity.

REFERENCES

- [1] E. Dahlman, S. Parkvall, and J. Skold, *5G NR: the next generation wireless access technology*. Academic Press, 2018.
- [2] (2021) Jammer-store. [Online]. Available: <http://www.jammer-store.com>
- [3] M. Wilhelm *et al.*, "Short paper: Reactive jamming in wireless networks: How realistic is the threat?" in *Proc. ACM Conference on Wireless Network Security (WiSec)*, Hamburg (Germany), Jun. 2011.
- [4] G. Berardinelli *et al.*, "Extreme communication in 6G: Vision and challenges for 'in-X' subnetworks," *IEEE Open Journal of the Communications Society*, vol. 2, pp. 2516–2535, 2021.
- [5] A. Chorti *et al.*, "Context-aware security for 6G wireless: the role of physical layer security," <https://arxiv.org/abs/2101.01536>, Jan. 2021.
- [6] W. Xu *et al.*, "Jamming sensor networks: attack and defense strategies," *IEEE Netw.*, vol. 20, no. 3, pp. 41–47, May-Jun. 2006.
- [7] T. T. Do *et al.*, "Jamming-resistant receivers for the massive MIMO uplink," *IEEE Trans. Inf. Forensics Security*, vol. 13, no. 1, pp. 210–223, Jan. 2018.
- [8] L. Chiarello *et al.*, "Jamming detection with subcarrier blanking for 5G and beyond in Industry 4.0 scenarios," in *Proc. IEEE International Symposium on Personal, Indoor and Mobile Radio Communications (PIMRC)*, Virtual Conference, Sep. 2021.
- [9] K. Grover, A. Lim, and Q. Yang, "Jamming and anti-jamming techniques in wireless networks: a survey," *Int. J. Ad Hoc and Ubiquitous Computing*, vol. 17, no. 4, pp. 197–215, 2014.
- [10] M. Alonzo *et al.*, "Cell-free and user-centric massive MIMO architectures for reliable communications in indoor factory environments," *IEEE Open Journal of the Communications Society*, vol. 2, pp. 1390–1404, 2021.
- [11] R1-1813177, "Scenarios, frequencies and new field measurement results from two operational factory halls at 3.5 GHz for various antenna configurations," Nokia, Tech. Rep., Nov. 2018.
- [12] 3rd Generation Partnership Project (3GPP), "Study on channel model for frequencies from 0.5 to 100 GHz," Tech. Rep., TR 38.901, Jun. 2018.
- [13] K. Brueninghaus *et al.*, "Link performance models for system level simulations of broadband radio access systems," in *Proc. IEEE International Symposium on Personal, Indoor and Mobile Radio Communications (PIMRC)*, Berlin (Germany), Sep. 2005.
- [14] G. Durisi, T. Koch, and P. Popovski, "Toward massive, ultrareliable, and low-latency wireless communication with short packets," *Proc. IEEE*, vol. 104, no. 9, pp. 1711–1726, Sep. 2016.
- [15] S. M. Kay, *Fundamentals of statistical signal processing: detection theory*. Prentice Hall, 1993.
- [16] B. Nadler, F. Penna, and R. Garello, "Performance of eigenvalue-based signal detectors with known and unknown noise level," in *Proc. IEEE International Conference on Communications (ICC)*, Kyoto (Japan), Jun. 2011.

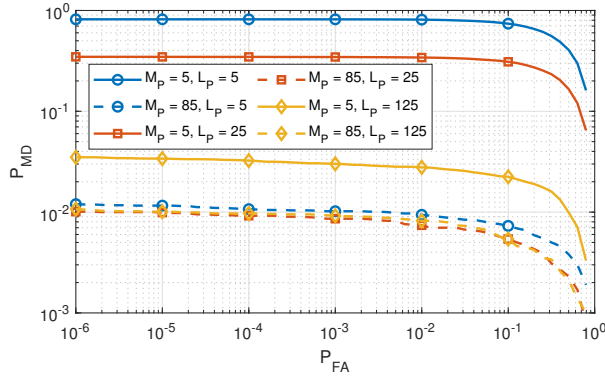


Fig. 7. P_{MD} versus P_{FA} for $N_{AP} = 16$, $B = 100$ MHz, and RLRT detector.

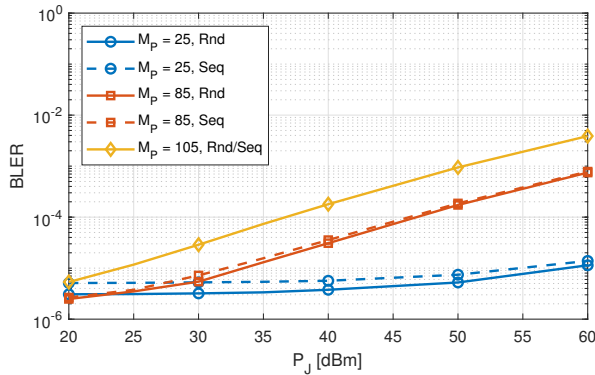


Fig. 8. BLER versus P_J for $N_{AP} = 1$, $B = 100$ MHz, and $L_P = 25$.

band and wide-band jammer), and RLRT detector. In this case, thanks to the larger number of available PRBs, a massive blanking approach can be implemented and, indeed, MD probability is lower with more blanked PRBs. Moreover, with massive blanking MD probability is similar across the different jamming strategies, thus allowing to better detect narrow-band jammers.

Regarding the comparison among the different mitigation strategies, we consider Fig. 8, which reports BLER as a function of P_J for for $N_{AP} = 1$, $B = 100$ MHz, random and sequential scheduling, $M_P = 25, 85, 105$, and $L_P = 25$. First, we notice that the scheduling-based mitigation works, although just a very small improvement is achieved by random scheduling when compared to the sequential one. Then, we observe a trade-off when applying frequency hopping: small M_P (large bandwidth for data transmission) provides better performance in most ranges, but frequency hopping (large M_P) starts obtaining better performance when the jamming power is low, under whose conditions lower BLER can also be achieved by the system. In other words, these results tell that frequency hopping becomes helpful as a jamming mitigation scheme mainly when reliability requirements with URLLC are stricter, otherwise the increase in SINR is not sufficient to even compensate for the reduced bandwidth.